Published in final edited form as:
J Biol Chem. 2008 February 29; 283(9): 5748–5759. doi:10.1074/jbc.M709288200.

A Novel Connexin43-interacting Protein, CIP75, Which Belongs to the UbL-UBA Protein Family, Regulates the Turnover of Connexin43[*,S]

Xinli Li[‡,1], **Vivian Su**[‡,1], **Wendy E. Kurata**[‡], **Chengshi Jin**[§], and **Alan F. Lau**[‡,¶,2]

[‡] Natural Products and Cancer Biology Program, Cancer Research Center of Hawaii, Honolulu, Hawaii 96813

[§] Department of Epidemiology and Biostatistics, University of California, San Francisco, San Francisco, California 94143

[¶] Department of Cell and Molecular Biology, John A. Burns School of Medicine, University of Hawaii at Manoa, Honolulu, Hawaii 96822

Abstract

The degradation of connexin43 (Cx43) has been reported to involve both lysosomal and proteasomal degradation pathways; however, very little is known about the mechanisms regulating these Cx43 degradation pathways. Using yeast two-hybrid, glutathione *S*-transferase pull-down, and co-immunoprecipitation approaches, we have identified a novel Cx43-interacting protein of ~75 kDa, CIP75. Laser confocal microscopy showed that CIP75 is located primarily at the endoplasmic reticulum, as indicated by the calnexin marker, with Cx43 co-localization in this perinuclear region. CIP75 belongs to the UbL (ubiquitin-like)-UBA (ubiquitin-associated) domain-containing protein family with a N-terminal UbL domain and a C-terminal UBA domain. The UBA domain of CIP75 is the main element mediating the interaction with Cx43, whereas the CIP75-interacting region in Cx43 resides in the PY motif and multiphosphorylation sites located between Lys^{264} and Asn^{302}. Interestingly, the UbL domain interacts with the S2/RPN1 and S5a/RPN10 protein subunits of the regulatory 19 S proteasome cap subunit of the 26 S proteasome complex. Overexpression experiments suggested that CIP75 is involved in the turnover of Cx43 as measured by a significant stimulation of Cx43 degradation and reduction in its half-life with the opposite effects on Cx43 degradation observed in small interference RNA knockdown experiments.

Gap junctions are plasma membrane channels constructed of connexins, which mediate the direct cell to cell communication of small molecules of <1000 Da, such as ions and regulatory molecules like Ca^{2+}, inositol 1,4,5-trisphosphate, and cAMP (1,2). Cx43[3] is one of the most ubiquitously expressed connexins, and Cx43 gap junctions are critical to various physiological

[*]This work was supported by Grant CA052098 from the National Institutes of Health (to A. F. L.), and predoctoral fellowship HIFW-29-96 (to C. J.) from the American Heart Association, Hawaii Affiliate.

[S]The on-line version of this article (available at http://www.jbc.org) contains supplemental Fig. S1.

[2]To whom correspondence should be addressed: Natural Products and Cancer Biology Program, Cancer Research Center of Hawaii, 651 Ilalo St., BSB 222L, Honolulu, HI 96813. Tel.: 808-586-2959; Fax: 808-587-0742; aflau@crch.hawaii.edu.
[1]Both authors contributed equally to this work.

[3]The abbreviations used are: Cx43, connexin43; ER, endoplasmic reticulum; UbL, ubiquitin-like; UBA, ubiquitin-associated; ERAD, ER-associated degradation; MDCK, Madin-Darby canine kidney cell; NRKe, normal rat kidney cell; GST, glutathione *S*-transferase; ALLN, *N*-acetyl-Leu-Leu-norleucinal; PBS, phosphate-buffered saline; PMSF, phenylmethylsulfonyl fluoride; siRNA, small interference RNA.

functions, such as rhythmic myocardial contractions (1,3,4), nerve and pancreas function (5), oocyte maturation (6), and development (7).

Unlike most membrane proteins, connexins exhibit an exceptionally high metabolic lability with half-lives ranging from 1.5 to 5 h (8–10). The rapid turnover of connexins has been observed in a wide variety of cultured mammalian cells (10,11), whole organs (12), and intact animals (13). Therefore, an efficient and highly regulated degradation mechanism is necessary to control the dynamic turnover of connexins. Both lysosome and proteasome proteolytic pathways have been implicated in connexin turnover in a variety of cell types (14–18) and under various pathological conditions (19,20); however, a clear understanding of specific mechanisms that may regulate the degradation of connexins by these two distinct pathways is limited. The proteasome degrades cytosolic and nuclear proteins with high turnover rates and plays a role in the ER-associated degradation (ERAD) of proteins. Pulse-chase analysis has revealed that proteasome inhibitors decrease the turnover rate of Cx43 in tissue culture cells (16,17) and in whole organs (12). It has also been shown that the ubiquitin proteasome pathway is involved in the degradation of Cx43 (15,18). Ubiquitinated Cx43 has been identified (21), and the ubiquitination of Cx43 has been found to affect Cx43 turnover and stability (16,18, 22,23). However, no connexin-specific ubiquitin ligase or the direct involvement of ubiquitination in ERAD of connexin has been reported.

Several proteins that interact with connexins have been reported to contribute to the regulation of gap junction assembly and turnover. The tight junction-associated protein, ZO-1, was implicated in the regulation of gap junction assembly by facilitating the formation of connexon hemichannel pairing (24,25). ZO-1 has also been reported to stabilize gap junctions possibly by interconnecting them with the actin cytoskeleton. Cx43 turnover was increased if Cx43 no longer interacted with ZO-1 (26). Cx43 can also interact directly with the actin cytoskeleton (27), which may play a role in the turnover of Cx43. Finally, we reported that a novel Rab GAP-like protein, CIP85, could interact with Cx43 and regulate its degradation, which appeared to be lysosome-dependent (28). Taken together, these data demonstrated that connexin-interacting proteins may be involved in the regulation of gap junction assembly, stabilization, and turnover.

Members of the UbL-UBA domain-containing protein family have been implicated in different biological functions, such as nucleotide excision repair (29,30), spindle pole body duplication (31), and protein degradation (32–34). Notably, the Rad23 and PLIC2 proteins have been reported to interact with the S2/RPN1 or S5a/RPN10 components of the 19 S subunit of the 26 S proteasome complex via their UbL domains (30,35,36). Moreover, the UBA domain can interact with monoubiquitin (37,38), multiubiquitin chains (34,36), and multiubiquitinated proteins (39,40). These data suggest that some UbL-UBA proteins might function as proteasome-substrate adaptors or carriers. The mechanism of Cx43 proteasomal degradation is poorly understood, and Cx43 has not been reported to interact directly with components of the proteasome. However, it has been suggested that adaptor proteins might be involved in the proteasomal degradation of Cx43 (18,23). A key attribute of a putative adaptor protein is the ability to bind both Cx43 and at least one proteasomal component; however, such possible adaptors have not been identified so far. Cx43 located in the ER can be dislocated from the ER and degraded by the proteasome through ERAD, which can be inhibited by cytosolic stressors, such as hyperthermia or sodium arsenite (23). It is not known if an adaptor protein or the 26 S proteasome itself is involved in the dislocation process for connexins.

In this work, we report the identification and characterization of a novel Cx43-interacting protein, CIP75, which contains an UbL-domain at its N terminus and an UBA domain at its C terminus. CIP75 also contains a PEST sequence and a heat shock chaperonin-binding domain. Significantly, CIP75 interacts with S2/RPN1 and S5a/RPN10 subunits of the 19 S proteasome

complex, and the UbL domain of CIP75 is essential for this interaction. The UBA domain of CIP75 interacts with Cx43 and this interaction appears to play a role in regulating the turnover of Cx43. These results suggest that CIP75 functions as an adaptor in the degradation of Cx43 via the proteasomal pathway.

EXPERIMENTAL PROCEDURES

Cell Culture and Transfection

Human embryonic kidney HEK293, human cervical carcinoma HeLa cells without endogenous Cx43 or stably infected with Cx43 (HeLa-Cx43), canine kidney epithelial MDCK with (MDCK-Cx43) or without endogenous Cx43, Cx43 knockout mouse fibroblasts (Cx43-KO), normal rat kidney (NRKe), and mouse sarcoma S180 cells with or without stably transfected L-cadherin (S180L) were cultured in high glucose Dulbecco's modified Eagle's medium (Invitrogen) supplemented with 10% fetal bovine serum, 20 mM L-glutamine, 100 units/ml penicillin, and 100 μg/ml streptomycin at 37 °C with 5% CO_2. Lipofectamine 2000 (Invitrogen), Effectene (Qiagen, Valencia, CA), or the Nucleofector (Amaxa, Gaithersburg, MD) was used for the transient expression of FLAG-CIP75 and/or Cx43 in HEK293, HeLa-Cx43, NRKe, and S180 cells. Transfected cells were harvested 24 or 48 h after transfection.

Plasmids and Antibodies

PCR-amplified FLAG-CIP75wt and its in-frame deletion mutants, FLAG-CIP75ΔUbL (deletion of the first 89 amino acid residues from the N terminus), and FLAG-CIP75ΔUBA (deletion of the last 44 amino acid residues from the C terminus) were cloned into the vectors pcDNA3.1 and pET28a (Invitrogen). PCR-amplified FLAG-UBA and FLAG-UbL were also cloned into the pET28a vector. To express glutathione *S*-transferase (GST)-Cx43 fusion proteins, Cx43CT and its deletion mutants were amplified by PCR and cloned into pGEX-KG at the BamHI and EcoRI sites. The accuracy of all constructs was verified by DNA sequencing. The following plasmids were also used in this study: pGEX-2TK-RPN10/S5a (Daniel Finley, Harvard Medical School, Boston, MA) and GST-RPN1/S2 (Youming Xie, Wayne State University). The following antibodies were used in this study: mouse anti-FLAG (Sigma); rat anti-FLAG (David Huang, The Walter and Eliza Hall Institute of Medical Research, Victoria, Australia); mouse anti-GST (Santa Cruz Biotechnology, Santa Cruz, CA); rabbit anti-actin (Sigma); mouse anti-human proteasome subunit S2 (Calbiochem, San Diego, CA); and mouse anti-Cx43 clones P2D12 and P4G9 (Paul Lampe, Fred Hutchinson Cancer Research Center, Seattle, WA). A rabbit antibody against the synthetic peptide (^{496}PRTSVPLAGSNSGSSA^{511}) of CIP75 (Washington Biotechnology, Simpsonville, MD) was developed. The synthetic peptide was identified as a highly antigenic region of CIP75 by using the Epitope Bioinformatics program. Antibody specificity was confirmed in peptide-blocking Western blots and immunoprecipitations. Additional reagents used were MG-132 and *N*-acetyl-Leu-Leu-norleucinal (ALLN) (Sigma) at a final concentration of 40 μM.

In Vitro GST/His Pull-down Assays

GST, GST-Cx43CT, GST-Cx43CT deletion mutants, GST-RPN1/S2, GST-RPN10/S5a, FLAG-CIP75, FLAG-CIP75ΔUbL, FLAG-CIP75ΔUBA, FLAG-UBA, and FLAG-UbL proteins were expressed in *Escherichia coli* BL21 cells grown to log phase. After induction with 2 mM isopropyl 1-thio-β-D-galactopyranoside for 3 h, the cells were harvested, resuspended in PBS supplemented with 2 mM PMSF, sonicated on ice six times for 25 s each, and lysates were clarified by centrifugation. For GST pull-down assays, lysates were incubated with glutathione-agarose beads, and the mixtures were rotated for 1 h at 4 °C. The beads were washed six times with lysis buffer, and the proteins were eluted with GST elution buffer containing 20 mM glutathione. For His pull-down assays, lysates with FLAG-CIP75 in pET28a (which contains a His tag) were incubated with cobalt beads for 2 h. After beads were washed,

precleared GST lysates were added and incubated with beads for 2 h. The beads were washed five times with binding buffer before boiling with sample buffer to release proteins. The proteins were resolved on SDS-containing 12% polyacrylamide gels and analyzed by immunoblotting with anti-FLAG, anti-GST, or anti-CIP75.

Co-immunoprecipitation

HEK 293 cells were transiently transfected with pcDNA3.1 vector, pcDNA-FLAG-CIP75, and pcDNA-Cx43 using Lipofectamine 2000, and incubated for 24 h, and the cells were harvested and lysed. For co-immunoprecipitation of endogenously expressed proteins, MDCK-Cx43 or S180 cells were grown to confluence, and the cells were lysed in 0.2% Nonidet P-40 lysis buffer (0.2% Nonidet P-40, 150 mM NaCl, 20 mM Tris-HCl, pH 8.0, 1 mM dithiothreitol, 5 μg/ml leupeptin, 5 μg/ml aprotinin, 2 mM PMSF, 50 mM NaF, 160 μM Na_3VO_4, 1 mM benzamidine), and the lysates were clarified by centrifugation at 100,000 × *g* for 20 min at 4 °C. Clarified supernatant proteins were immunoprecipitated with monoclonal anti-FLAG, anti-GST, anti-Cx43 antibody, or a control normal mouse serum. The immune complexes were collected with protein A/G-agarose beads, washed six times with 0.2% Nonidet P-40 lysis buffer, and the proteins released from the beads by boiling for 5 min in SDS-PAGE sample buffer. The proteins were analyzed by SDS-PAGE and immunoblotting for Cx43 and CIP75.

Metabolic Labeling

For endogenous CIP75 immunoprecipitation, cells were rinsed once with methionine-free medium and radiolabeled in the same medium with [^{35}S]methionine/cysteine (Expre^{35}S^{35}S, PerkinElmer Life Sciences) at 100 μCi/ml for 5 h. The cells were rinsed in cold PBS and lysed in radioimmune precipitation assay buffer (150 mM NaCl, 1% sodium deoxycholate, 1% Triton X-100, 0.1% SDS, 10 mM Tris, pH 7.2) supplemented with 1 mM dithiothreitol, 2 mM PMSF, 50 μg/ml benzamidine, 10 μg/ml aprotinin, and 10 μg/ml leupeptin. After centrifugation, the supernatant was immunoprecipitated with CIP75 antibody for 1 h at 4 °C and incubated with *Staphylococcus aureus* for 30 min. The immune complexes were collected after washing four times with radioimmune precipitation assay buffer, denatured by boiling in SDS-PAGE sample buffer, and the proteins resolved on a SDS-containing 10% polyacrylamide gel.

RNA Interference and Pulse-chase

CIP75 gene expression was reduced using *in vitro* synthesized small interfering RNA duplexes. *In vitro* transcription was performed by using the AmpliScribe T7 High Yield Transcription kit (Epicenter Technologies, Madison, WI). Desalted DNA oligonucleotide primers were ordered from IDT (Coralville, IA). The CIP75 sequence targeted by the siRNA-CIP75 was 5′-AAGGAGG-GCATTATACCCTCCTATAGTGAGTCGTATTACC-3′. Specificity for the CIP75 mRNA was verified by the BLAST search in the NCBI data base. Random siRNA controls (siRNA-CL) were prepared by four nucleotide replacement of siRNA-CIP75. siRNAs were transfected into cells using Lipofectamine 2000 or siLentfect lipid (Bio-Rad), and the cells were harvested at 24 h after the second transfection.

For pulse-chase experiments, cells were transfected with either a vector only control, CIP75wt, siRNA-CIP75, or random control siRNA-CL. Cells were rinsed once with methionine-free medium and radiolabeled in the same medium with [^{35}S]methionine/cysteine (Expre^{35}S^{35}S) at 100 μCi/ml for 1 h. Radiolabeled cells were chased in Dulbecco's modified Eagle's medium supplemented with 2 mM methionine for 3 and 6 h. The cells were rinsed in cold PBS and lysed in radioimmune precipitation assay buffer supplemented with 1 mM dithiothreitol, 50 mM NaF, 160 μM Na_3VO_4, 1 mM PMSF, 50 μg/ml benzamidine, 10 μg/ml pepstatin, and 10 μg/ml leupeptin. After centrifugation, the supernatant was immunoprecipitated with Cx43 antibody for 1 h at 4 °C and incubated with protein A/G-agarose beads (Santa Cruz Biotechnology, Santa Cruz, CA). The immune complexes were collected after washing six

times with radioimmune precipitation assay buffer and denatured in SDS-PAGE sample buffer, and the proteins were resolved on a SDS-containing 12% polyacrylamide gel. The gel was dried, and the radiolabeled proteins were visualized with a Cyclone phosphorimaging device (Packard Instrument, Meriden, CT). Protein degradation rate is expressed as $t_{½}$, the time for degradation of 50% of the labeled protein. The half-life data were expressed as the mean ± S.D. of three independent experiments.

Laser Scanning Confocal Microscopy

NRKe cells were transiently transfected with pcDNA-FLAG-CIP75. 24 h after transfection, cells were fixed in cold 80% methanol/20% acetone for 30 min at −20 °C and washed thrice with 0.1% Triton X-100 in PBS (PBSTx) for 5 min each. The cells were then blocked with 5% NGS and 1% bovine serum albumin in PBSTx for 30 min prior to incubation with mouse anti-Cx43 antibody, rat anti-FLAG antibody, and rabbit anti-calnexin antibody in blocking solution for 1 h. After three 5-min washes with PBS, the cells were incubated with goat anti-mouse Alexa 594, goat anti-rat Alexa 488, and goat anti-rabbit Alexa 647-conjugated secondary antibodies (Molecular Probes, Eugene, OR) for 1 h, then washed three times with PBS. The cells were mounted on slides with Prolong Antifade reagent (Molecular Probes, Eugene, OR), and the subcellular localization of Cx43, CIP75, and calnexin was examined using a TCS SP5 AOBS confocal microscope (Leica).

RESULTS

Characterization of a Novel Cx43-interacting Protein CIP75 with UbL and UBA Domains

The yeast two-hybrid system was applied to identify Cx43-interacting peptides (41,42). The cytoplasmic tail of Cx43 (Leu^{222}–Ile^{382}, Cx43CT), fused to the LexA DNA-binding domain (LexA-Cx43CT), was used as bait in a two-hybrid screen of a 9- to 10-day mouse embryo cDNA library (41,43). Forty-two positive library clones were identified and further tested for interaction by directed yeast two-hybrid assays. The ability of fifteen of the selected positive cDNA clones to interact with the Cx43CT was tested in additional directed two-hybrid assays (41). One relatively strong interacting clone, CAD6 (a portion of CIP75), was selected for further characterization in this study and used to isolate the full length CIP75 cDNA from an oligo-dT primed cDNA library prepared from a 16-day mouse embryo (28).

CIP75 has 596 amino acids and exhibited high amino acid sequence homology (75%) with the human A1Up protein (44). The secondary structure analysis of the CIP75 deduced amino acid sequence revealed that CIP75 contains a conserved ubiquitin-like domain (UbL, Ile^{13}–Ala^{89}) at its amino terminus and an ubiquitin-associated domain (UBA, Phe^{554}–Ser^{593}) at its C terminus (Fig. 1). CIP75 also contains a heat shock chaperonin-binding domain from amino acid Pro^{188} to Glu^{255}. A possible PEST sequence was also identified in CIP75 from Arg^{320} to Val^{353}. PEST sequences have been shown to direct the ubiquitination and subsequent degradation of proteins undergoing rapid turnover (45). The general domain organization of CIP75 showed high similarity to the human proteins A1Up, Rad23A, Rad23B, PLIC1, the mouse proteins Rad23A, Rad23B, PLIC1, and the yeast protein DSK2 (Fig. 1). All of these proteins contain one UbL domain and at least one UBA domain; thus, CIP75 is potentially a member of this UbL-UBA domain-containing protein family.

To investigate the possible function of CIP75, the UbL and UBA domains of CIP75 were aligned with those of human A1Up, PLIC1, Rad23A, Rad23B, mouse PLIC1, Rad23A, Rad23B, and yeast DSK2 (Fig. 2). The UbL domain of CIP75 (Ile^{13}–Ala^{89}) showed high homology with that of the A1Up, PLIC1, Rad23A, Rad23B, and DSK2 proteins (Fig. 2*A*), with the UbL domain of the A1Up protein showing the highest identity at 97% (Fig. 2*A*). CIP75 contained nearly all of the conserved amino acid residues of the UbL domain present in the

UbL-UBA protein family (Fig. 2*A*). Significantly, the CIP75 UbL domain contained the amino acid residues (Thr^{19}, Lys^{38}, Lys^{54}, Ile^{55}, Ala^{57}, Ile^{60}, Val^{81}, and Ile^{82}), which were shown to be responsible for the interaction of the UbL domain of the ubiquitin-like proteins with the proteasome S5a subunit (46). The UBA domain of CIP75 (Phe^{554}–Ser^{593}) also had high homology with the UBA domains of A1Up, PLIC1, DSK2 and the two UBA domains of Rad23A and Rad23B (Fig. 2*B*). The CIP75 UBA domain showed 100 and 95% identity to those of human A1Up and PLIC1, respectively (Fig. 2*B*). The similarity among the UBA domains of these proteins was higher than that of the UbL domains, which suggested that the conservation of the UBA domain was greater than that of the UbL domain (Fig. 2*B*).

CIP75 Interacts with Cx43 through Its UBA Domains

The UBA domains of Rad23 and DSK2 have been shown to bind ubiquitin and polyubiquitinated proteins (39,40,47). To identify the Cx43 interacting-domain of CIP75, two deletion mutants of CIP75, lacking either the UbL or UBA domain, were fused to the FLAG epitope tag (Fig. 3*A*). The Cx43 C-terminal region, fused to GST (GST-Cx43CT), the wild-type FLAG-CIP75 or the CIP75 mutants lacking either the UbL (CIP75ΔUbL) or the UBA domains (CIP75ΔUBA) were expressed in bacteria (Fig. 3*A*). Equal amounts of whole cell lysates expressing these proteins were incubated with glutathione-agarose beads, and the protein complexes that were bound to the GST fusion proteins were resolved by SDS-PAGE and examined by immunoblotting with the FLAG antibody. The GST pull-down results showed that both the full-length CIP75wt (Fig. 3*B*, *lane 2*) and the UbL-deletion mutant (CIP75ΔUbL) (Fig. 3*B*, *lane 4*) interacted with the GST-Cx43CT. In contrast, the interaction of the UBA-deletion mutant (CIP75ΔUBA) with GST-Cx43CT was nearly undetectable (Fig. 3*B*, *lane 5*). Importantly, FLAG-CIP75 was not detected in the GST-only control pull down (Fig. 3*B*, *lane 3*). These results demonstrated that CIP75 can interact with Cx43CT *in vitro*, and the UBA domain of CIP75 is likely a major domain that dictates the interaction with Cx43. It is also possible that a second region of CIP75 corresponding to the CAD6 region, isolated in the original yeast two-hybrid screen, can interact with Cx43, but the interaction appeared to be much weaker than that of the UBA domain (41).[4] Interestingly, because bacteria do not exhibit protein ubiquitination (48), the interaction between CIP75 and GST-Cx43CT may be ubiquitin-independent, and perhaps the UBA domain of CIP75 interacts with non-ubiquitinated GST-Cx43CT protein.

The yeast two-hybrid and GST pull-down results demonstrated that Cx43CT interacts with CIP75. To investigate whether full-length Cx43 might interact with CIP75 in intact cells, HEK293 cells were co-transfected with Cx43 and FLAG-CIP75. Cell lysates were immunoprecipitated with either the Cx43 or FLAG antibody, and the proteins were immunoblotted with antibody against the reciprocal protein to detect the interaction. Normal mouse serum and the GST antibody were used as immunoprecipitation negative controls. CIP75 was detected in Cx43 immunoprecipitates (Fig. 3*C*, *lane 5*), and Cx43 was detected in the reciprocal FLAG-CIP75 immunoprecipitate (Fig. 3*C*, *lane 2*). The normal mouse serum and GST antibody controls did not show similar co-immunoprecipitation results (Fig. 3*C*, *lanes 1*, *3*, *4*, and *6*). These data demonstrated that full-length Cx43 can interact with CIP75 when both proteins are co-expressed in HEK293 cells.

To investigate if the UBA domain is essential for the CIP75 interaction with Cx43, HeLa-Cx43 cells were transfected with FLAG-CIP75wt, and FLAG-CIP75ΔUBA and FLAG-[4] X. Li, V. Su, W. E. Kurata, C. Jin, and A. F. Lau, unpublished data. CIP75ΔUbL deletion mutants. Equal amounts of whole cell lysates were immunoprecipitated with either FLAG or Cx43 antibodies, and the presence of Cx43 in the immunoprecipitates was detected by immunoblotting with the Cx43 antibody. We discovered that the interaction between Cx43 and CIP75 was greatly reduced in the HeLa-Cx43 cells transfected with the CIP75ΔUBA deletion mutant (Fig. 3*D*,

lane 4), whereas the interaction between Cx43 and CIP75ΔUbL deletion mutant was comparable to that for the Cx43 and CIP75wt (Fig. 3*D*, *lanes 2* and *6*). The expression of Cx43 and FLAG-CIP75 proteins in these cells is shown in the *right panel* of Fig. 3*D*. These results suggested that the UBA domain is essential for the interaction between full-length CIP75 and Cx43 in intact cells.

A rabbit polyclonal antibody against CIP75 was prepared to investigate the interaction between CIP75 and Cx43 expressed at endogenous levels in cells. We first examined the ability of the resulting antibody to recognize endogenous CIP75 in various cell lines: Cx43 knockout cells, HEK293 cells, parental MDCK cells, MDCK-Cx43 cells, HeLa cells, HeLa cells stably expressing Cx43, S180, and S180L cells, and NRKe cells. Endogenous CIP75 (~75-kDa band) was detected at significant levels in the S180 and S180L cells (Fig. 3*E*, *lanes 8* and *9*), and it was also found at lower levels in the remaining cells (Fig. 3*E*, *lanes 2–7* and *10*). Preimmune rabbit serum did not recognize endogenous CIP75 in either Cx43 knockout or NRKe cells (Fig. 3*E*, *lanes 1* and *11*). Furthermore, the CIP75 band was specifically diminished by preincubating the antibody with competing immunizing peptide (supplemental Fig. S1A, *lanes 2–4*). In addition, the CIP75 antibody specifically recognized the FLAG-CIP75 protein expressed in bacteria (supplemental Fig. S1B, *lane 1*), which was also blocked by preincubating the antibody with immunizing peptide prior to incubation with the blot (supplemental Fig. S1B, *lane 2*). To investigate the interaction of endogenous CIP75 with Cx43, we selected the MDCK-Cx43 cell line, which contained a moderate level of both endogenous CIP75 and Cx43. Whole cell lysates were immunoprecipitated with either Cx43 or CIP75 antibodies, and the associated protein was detected by immunoblotting using the reciprocal antibody. CIP75 antibody immunoprecipitates contained Cx43, and the reciprocal immunoprecipitation with Cx43 antibody revealed the presence of CIP75 (Fig. 3*F*, *lanes 3* and *4*). Cx43 and CIP75 were not detected in the immunoprecipitates prepared using either GST antibody or preimmune rabbit serum (Fig. 3*F*, *lanes 1* and *2*). These results not only confirmed the previous *in vitro* interaction data, but importantly, indicated that endogenous CIP75 and Cx43 interacted with each other.

The Region of Cx43 Containing Multiple Phosphorylation Sites, a Proline-rich Region, and a WW-binding Domain Is Required for Binding to CIP75

The C-terminal region of Cx43 was used as bait in the yeast two-hybrid screening, which originally identified a fragment of CIP75 (41,42). However, to refine the region of Cx43 required for CIP75 binding, various deletion mutants of GST-Cx43CT were prepared, and their ability to bind CIP75 was tested by *in vitro* pulldown experiments (Fig. 4*A*). FLAG-CIP75 clearly interacted with Cx43CTwt (residues Val^{236}–Ile^{382}) and the Cx43CT-302 (containing residues Val^{236}–Asn^{302}) deletion mutant (Fig. 4*B*, *lanes 5* and *4*). However, the Cx43CT-263 (residues Val^{236}–Pro^{263}) and Cx43CT-252 (residues Val^{236}–Gly^{252}) deletion mutants failed to interact with CIP75 (Fig. 4*B*, *lanes 2* and *3*), which indicated that the region between Lys^{264}–Asn^{302} of Cx43 was necessary for Cx43 binding to CIP75. To confirm this prospect, the Lys^{264}–Asn^{302} region of Cx43 was fused to GST and used in pulldown assays. As shown in Fig. 4*C* (*lane 4*), this region was sufficient to interact with FLAG-CIP75 *in vitro*. This result is very interesting because this region of Cx43 contains multiple phosphorylation sites (Tyr^{265}, Ser^{279}, and Ser^{282}), a proline-rich region (Pro^{277}–Pro^{284}), and an overlapping WW-binding domain (Ser^{282}–Tyr^{286}). Proline-rich regions and the WW-binding domains of the rH1 and CiC-5 proteins have been demonstrated to be involved in interactions with ubiquitin-protein ligases (49,50), which suggests that CIP75 may regulate the turnover of Cx43 involving ubiquitination.

CIP75 Co-localizes with Cx43 in Selected Subcellular Compartments

The biochemical demonstration of the CIP75-Cx43 interaction predicted that subpopulations of these proteins might co-localize in subcellular compartments. To substantiate this prediction,

NRKe cells were transiently transfected with FLAG-CIP75 and co-localization was examined by laser scanning confocal microscopy using Cx43 and FLAG antibodies. Cx43 was clearly evident at the cell periphery in punctate stainings reminiscent of gap junction plaques and in the cytoplasm (Fig. 5, *B* and *G*). CIP75 was localized primarily to the cytoplasmic, perinuclear region (Fig. 5, *A* and *F*). Interestingly, expression of CIP75 caused varying levels of Cx43 accumulation in the cytoplasm that were not seen in untransfected cells, and the cytoplasmic Cx43 co-localized with CIP75 (Fig. 5, *C* and *H*). In addition, the perinuclear/cytoplasmic localization of CIP75 and Cx43 was demonstrated to be at or around the ER based upon a similar pattern of localization and partial co-localization with the ER-specific marker calnexin (Fig. 5, *D*, *I*, *E*, and *J*). The apparent co-localization of CIP75 and Cx43 in the ER region is consistent with their previously demonstrated ability to interact biochemically.

CIP75 Stimulates the Degradation of Cx43

Because several UbL-UBA domain-containing proteins, such as Rad23 and PLIC1, have been implicated as adaptors involved in delivering ubiquitinated substrates to the proteasome (32, 51), we investigated if CIP75 affected the stability of Cx43. HeLa-Cx43 cells were transfected with FLAG-CIP75 or its deletion mutants, equal amounts of whole cell lysates were resolved by SDS-PAGE, and the levels of Cx43 were assayed by immunoblotting. The expression of CIP75wt in HeLa-Cx43 cells was associated with a modest, but statistically significant ($p < 0.01$), decrease of Cx43 levels of ~30% compared with the vector-only transfected HeLa-Cx43 cells (Fig. 6*A*, *lane 4*, and Fig. 6*B*). It is important to note that this 30% decrease was observed with an average transfection efficiency of CIP75wt and its deletion mutants into HeLa-Cx43 cells of ~70% (data not shown). The CIP75ΔUBA deletion mutant, which does not interact with Cx43, failed to diminish Cx43 levels, compared with the cells expressing CIP75wt (Fig. 6*A*, *lane 3*, and Fig. 6*B*), which suggested that the interaction of CIP75 with Cx43 through the UBA domain is essential for the ability of CIP75 to regulate Cx43 levels in these cells. The CIP75ΔUbL deletion mutant also did not diminish Cx43 levels, which may be due to the potential inability of CIP75ΔUbL to interact with components of the proteasome (Fig. 6*A*, *lane 2*, and Fig. 6*B*). It is possible that the CIP75ΔUbL mutant may function as a dominant-negative mutant of CIP75 because its ability to interact with Cx43 is intact, but it may not interact with proteasome components and thus would be unable to facilitate the proteasome degradation of Cx43.

Depression of CIP75 Levels by siRNA Elevates the Levels of Endogenous Cx43

To further examine the effect of CIP75 on Cx43 degradation, a CIP75 siRNA (siRNA-CIP75), corresponding to the CIP75 nucleotide sequence of residues 902–921 was prepared and tested for the ability to reduce CIP75 levels in HeLa-Cx43 and S180 cells. The siRNA treatment of HeLa-Cx43 cells, which express a low level of endogenous CIP75 (Fig. 3*E*), reduced CIP75 levels by ~70% in these cells (Fig. 6*A*, *bottom panel*, *lane 2*). Notably, the reduction of the endogenous CIP75 in HeLa-Cx43 cells also produced a statistically significant increase in the Cx43 protein level of ~20%, compared with the random siRNA and vector-only transfected control cells (Fig. 6*A*, *top panel*, *lane 5*, and Fig. 6*B*). The random siRNA control, which did not reduce the level of endogenous CIP75 (Fig. 6*A*, *bottom panel*, *lane 3*), left Cx43 levels unaffected (Fig. 6*A*, *top panel*, *lane 6*, and Fig. 6*B*). To expand these studies, S180 cells were employed, which endogenously express high levels of Cx43 and CIP75. The siRNA treatment reduced CIP75 levels to ~30% of the random siRNA control level in S180 cells (Fig. 6*C*, *top panel*, *lane 2*, and Fig. 6*D*, *left panel*). The siRNA-induced reduction in endogenous CIP75 levels was associated with a significant increase of nearly 55% in the level of Cx43 (Fig. 6*C*, *middle panel*, *lane 2*, and Fig. 6*D*, *right panel*). Importantly, the random siRNA control did not affect CIP75 or Cx43 levels (Fig. 6*C*, *top* and *middle panels*, *lane 3*, and Fig. 6*D*). These combined results in two different cell lines suggested that the expression of CIP75 was associated with decreased Cx43 levels.

To determine if the effect of CIP75 on the levels of Cx43 involved an increase in the Cx43 turnover rate, pulse-chase experiments were conducted using HeLa-Cx43 cells. Effects of an increased level of CIP75 on Cx43 levels were examined in these cells by the transient transfection and overexpression of exogenous CIP75. HeLa-Cx43 cells transfected with vector only showed a Cx43 half-life of ~2.9 h (Fig. 6*E*). Overexpression of exogenous CIP75 reduced the half-life of Cx43 to ~2.4 h (Fig. 6*E*). Remarkably, the introduction of the CIP75 siRNA, which would be expected to reduce both exogenous and endogenous CIP75 levels, significantly increased the half-life of Cx43 to around 4.8 h (Fig. 6*E*). This elevated Cx43 half-life can be compared with that in the random CIP75 siRNA and vector control cells, which exhibited a Cx43 half-life of ~2.9 h (Fig. 6*E*). Thus, the ability of CIP75 to stimulate a reduction in Cx43 levels was associated with an increase in turnover rate of Cx43.

Proteasomal Degradation May Be Involved in CIP75-regulated Cx43 Degradation

To investigate if the CIP75-associated degradation of Cx43 is mediated by proteasomes, HeLa-Cx43 cells transfected with either CIP75wt or a vector control were treated 24 h after transfection with the proteasome inhibitor, MG-132, for 4 h. MG-132 induced a dose-dependent block of Cx43 degradation associated with expression of CIP75, with the inhibition effective at a concentration of MG-132 as low as 20 μM (Fig. 7, *A* and *B*). Similar results were also observed using the proteasome inhibitor ALLN (data not shown). These results suggested that the proteasome is a major pathway by which CIP75 stimulates the degradation of Cx43. These observations, combined with the previous report of the degradation of Cx43 by proteasomes in ERAD (23), our discovery of CIP75 co-localized with Cx43 at the ER, and its structural similarity to other UBA-UbL domain proteins, which may function as adaptors for proteasome substrates, suggested that CIP75 may be involved in the dislocation of Cx43 from the ER and its subsequent degradation by the proteasome.

CIP75 Interacts with the S2/RPN1 and S5a/RPN10 Subunits of the 19 S Proteasome Complex via Its UbL Domain

The experiments using the MG-132 inhibitor suggested the involvement of proteasomes in the CIP75-associated degradation of Cx43. Because several UbL-UBA domain-containing proteins have been reported to interact with the S2/RPN1 and S5a/RPN10 subunit proteins of the 19 S regulatory particle of the proteasome (35,52), we were interested in establishing if CIP75 also interacted with these 19 S proteasome proteins. FLAG-CIP75wt, FLAG-CIP75ΔUBA, and FLAG-CIP75ΔUbL, and the isolated UBA and UbL domains (FLAG-UBA and FLAG-UbL, Fig. 8*A*) were used in GST pulldown assays against bacterially expressed and purified GST-S2/RPN1 and GST-S5a/RPN10 proteasomal proteins. The S5a/RPN10 protein interacted with CIP75wt, the CIP75ΔUBA deletion mutant, and the isolated UbL domain (Fig. 8*B*, *lanes 2*, *4*, and *6*), but not with the CIP75ΔUbL deletion mutant or the isolated UBA domain (Fig. 8*B*, *lanes 3* and *5*). Similar results were obtained in GST pulldown assays between the S2/RPN1 subunit and CIP75 (Fig. 8*C*). In addition, the S2/RPN1 subunit interacted with the isolated UbL domain, but not the UBA domain (Fig. 8*C*, *bottom panel*, *lanes 3* and *4*). These data indicated that CIP75 can interact *in vitro* with the RPN10 and RPN1 proteasomal subunits through its UbL domain, as has been reported for other UbL-UBA domain-containing proteins (35,46,52).

To further explore the interaction between CIP75 and the proteasome in intact cells, FLAG-CIP75 was transiently expressed in HeLa-Cx43 cells, and whole cell lysates were immunoprecipitated with either the S2/RPN1 or FLAG antibody, followed by immunoblotting with the reciprocal antibody. These results showed that CIP75 co-immunoprecipitated with S2/RPN1 (Fig. 8*D*, *lane 3*), and, in the reciprocal reaction, the S2/RPN1 protein co-immunoprecipitated with CIP75 (Fig. 8*D*, *lane 4*). These data not only confirmed the *in vitro*

GST pulldown assay results, but importantly, showed that CIP75 can interact with the S2/RPN1 proteasome protein in intact cells.

DISCUSSION

In the present work, we demonstrate that CIP75 is a novel Cx43-interacting protein, which confirmed results from our earlier yeast two-hybrid screen that CAD6, comprising a region of CIP75, interacted with the C-terminal region of Cx43 (42). The conclusion that CIP75 is a Cx43-interacting protein was supported by results from several different experimental approaches. First, the *in vitro* GST pulldown assays of purified GST-Cx43CT and CIP75 expressed in bacteria showed the interaction between the full-length CIP75 and Cx43CT (Fig. 3*B*). Second, co-immunoprecipitation of CIP75wt and Cx43 co-expressed in HEK293 and HeLa-Cx43 cells confirmed their interaction (Fig. 3, *C* and *D*). Third, co-immunoprecipitation assays demonstrated the interaction between CIP75 and Cx43 expressed endogenously in MDCK cells (Fig. 3*F*). Finally, as predicted from these biochemical studies, laser scanning confocal microscopy showed that some subpopulations of CIP75 and Cx43 co-localized in NRKe cells, principally at calnexin-positive perinuclear regions, indicative of the ER (Fig. 5). Importantly, overexpression and siRNA experiments revealed that CIP75 stimulated the degradation of Cx43 mediated by the proteasomal processing system, which may involve the dislocation of Cx43 from the ER and its degradation by the proteasome in the cytoplasm.

The presence of UbL and UBA domains suggested that CIP75 belongs to the newly emerging UbL-UBA domain-containing protein family. The UbL-UBA proteins have been shown to play important roles in the ubiquitin-proteasome protein degradation pathway (33,34,39,40, 53). The UbL-UBA protein, Rad23, has been implicated as an adaptor or “shuttle factor” for the translocation of ubiquitinated protein substrates from membrane and/or cytoplasmic locations and the docking to the 26 S proteasome for degradation (39,54). Rad23 acts on proteins such as Rad4, the γ-aminobutyric acid receptor, and a cyclin-dependent kinase inhibitor (39,53–55). Similarly, the yeast DSK2 protein has also been implicated as an adaptor in the ubiquitin-proteasome protein degradation pathway via its UbL and UBA domains (40). The principal function of the UbL domain is to mediate the interaction between an UbL-UBA protein and elements of the proteasome (35,52,56,57). The UBA domain of UbL-UBA proteins has a general capacity to bind ubiquitinated proteins *in vitro*, but it shows substrate specificity *in vivo*, which may explain why several UbL-UBA proteins have been identified so far (58). We noted recently that CIP75 is 100% identical to the mouse UBIN protein, which was reported to localize to the ER and interact with HSP47, an ER chaperone, through UBIN amino acids 140–254, corresponding to the CIP75 chaperonin-binding domain (Fig. 1) (59).

The observation that CIP75 stimulated the degradation of Cx43, largely via the proteasomal system, prompted an important question: What is the mechanism by which CIP75 effects these changes in Cx43 metabolism? Based upon models described for other UbL-UBA proteins, such as Rad23, our data suggested the hypothesis that CIP75 may function as an adaptor or shuttle factor that facilitates the extraction or dislocation of Cx43 from intracellular sites, such as the ER, for proteasomal degradation. This putative adaptor function of CIP75 may operate first to dislocate either unfolded or misfolded Cx43 specifically from the ER, followed by the transfer of Cx43 to the 26 S proteasome for efficient degradation in the process known as ER-associated degradation or ERAD (60,61). This suggestion was prompted by the original observations by Van Slyke and Musil (23) that Cx43 is subject to ERAD in S180, Chinese hamster ovary, and NRK cells. Cx43 was shown to be ejected or dislocated from the ER into the cytosol in an intact form in the presence of the proteasomal inhibitor, ALLN, but was subject to rapid degradation upon restoration of proteasomal function by removal of the inhibitor (23). The dislocation of Cx43 from the ER was markedly reduced by cytosolic stress induced by oxidative (sodium arsenite) or hyperthermal treatments leading to an increase in gap junction

formation and gap junctional communication. The notion that CIP75 may function at the ER is consistent with our observations that subpopulations of CIP75 appear to co-localize with increased amounts of Cx43 in calnexin-positive perinuclear regions (Fig. 5). The increased cytoplasmic Cx43 that resulted from CIP75 expression corroborates the biochemical results where CIP75 expression leads to decreased amounts of Cx43 (Fig. 6). Because the decreased Cx43 level is due to proteasomal degradation, it is possible that the increased cytoplasmic Cx43 represents Cx43 that is being targeted for proteasomal degradation through CIP75. Van Slyke and Musil (23) proposed that 26 S proteasomes are recruited to the ER by presumably misfolded Cx43 destined for ERAD, with the proteasome participating in the dislocation of Cx43 from the ER membrane. As far as we know, Cx43 has not been reported to interact directly with the proteasome or its components; thus, our modification of this model postulates that CIP75 may serve as an "adaptor": utilizing the UBA domain at its C terminus to bind to the C-terminal region of Cx43, which is localized to the cytosolic face of the ER membrane, and its UbL domain to interact with 19 S proteasomal subunits, such as the S2/RPN1 and the S5a/RPN10 proteins. The failure of the CIP75ΔUBA and CIP75ΔUbL deletion mutants to foster Cx43 degradation presumably reflects their inability to interact with either Cx43 or the 19 S proteasomal elements, respectively.

Interestingly, the CIP75-interacting domain in the C-terminal region of Cx43 is localized primarily to the domain between Lys^{264}–Asn^{302}, which contains a proline-rich motif that conforms to the consensus PY motif (*X*PP*X*Y), a WW-binding domain, and several serine and tyrosine phosphorylation sites. Several ion channels interact with ubiquitin ligases via PY motif/WW domain interactions, which lead to their ubiquitin-associated proteasomal degradation (49,50,62–64). Ubiquitination and proteasomal degradation of Cx43 has also been reported in different cell types and physiological states (15,22,65). Recently, Cx43 was reported to interact with the Nedd4 ubiquitin ligase (66). Knockdown of Nedd4 by siRNA resulted in a corresponding increase in the number of gap junction plaques at interjunctional plasma membranes (66). The WW domains of Nedd4 were found to bind Cx43, and in particular, the WW2 domain of Nedd4 interacted with the S^{282}PPGY^{286}PY motif located in the C-terminal region of Cx43 (66). It is possible that CIP75 may also function as a cofactor for anubiquitinligaselikeNedd4intheregulationofubiquitination-dependent degradation of Cx43. The interaction between CIP75 and Cx43 may modulate the interaction between Cx43 and such ubiquitin ligases. Further studies are required to address the ubiquitination state of CIP75-interacting Cx43 to assess this possibility. It has also been reported that phosphorylation of Cx43 stimulates its ubiquitination and subsequent degradation (20,65) and that ubiquitination of Cx43 may be regulated by both protein kinase C and mitogen-activated protein kinase pathways (65).

Several Cx43-interacting proteins have been shown to affect the turnover of Cx43 (25,28). It would be interesting to determine if the binding of one Cx43-interacting protein affected the binding affinity of another Cx43-interacting protein and its biological functions. Given the nature of gap junction assembly, even a modest change of connexin levels at the plasma membrane can result in a rapid change in gap junction plaque formation and cell communication (23). Thus, the trafficking and turnover of connexin must be tightly regulated in response to different physiological status. The distinct roles of the Cx43-interacting proteins in regulating the turnover of Cx43 might be different in response to different cellular stresses and signals. CIP75 may possibly interact with other cellular proteins, which in turn may affect the interaction of CIP75 with Cx43 and the proteasome. The UbL domain of Rad23 has been shown to directly interact with ufd2 (E4), and this interaction affects the UBA domain interaction with its target protein and the subsequent proteasome delivery and degradation (32). Thus, it is possible that other CIP75-interacting proteins may regulate the binding affinity of CIP75 with Cx43 and the proteasome, affecting its function in the proteasomal degradation process.

Heat-shock stress has been shown to stimulate the degradation of Cx43 (67). Interestingly, CIP75 has a heat-shock chaperonin-binding domain, which may play a role in the heat-shock-induced degradation of Cx43. An interesting question to be addressed in future studies is whether or not CIP75 is regulated in response to physiological stresses. It is possible that changes in the level or post-translational modification of CIP75 may affect the retrotranslocation and the ubiquitination and degradation of Cx43 that can lead to changes in gap junctional communication.

Supplementary Material

Refer to Web version on PubMed Central for supplementary material.

Acknowledgments

We thank Drs. D. Finley, Y. Xie, D. Huang, and P. Lampe for providing molecular and immunological reagents.

References

1. Goodenough DA, Goliger JA, Paul DL. Annu Rev Biochem 1996;65:475–502. [PubMed: 8811187]
2. Kumar NM, Gilula NB. Cell 1996;84:381–388. [PubMed: 8608591]
3. Beyer EC, Paul DL, Goodenough DA. J Membr Biol 1990;116:187–194. [PubMed: 2167375]
4. Willecke K, Eiberger J, Degen J, Eckardt D, Romualdi A, Guldenagel M, Deutsch U, Sohl G. Biol Chem 2002;383:725–737. [PubMed: 12108537]
5. Sohl G, Maxeiner S, Willecke K. Nat Rev Neurosci 2005;6:191–200. [PubMed: 15738956]
6. Sela-Abramovich S, Edry I, Galiani D, Nevo N, Dekel N. Endocrinology 2006;147:2280–2286. [PubMed: 16439460]
7. Wei CJ, Xu X, Lo CW. Annu Rev Cell Dev Biol 2004;20:811–838. [PubMed: 15473861]
8. Darrow BJ, Laing JG, Lampe PD, Saffitz JE, Beyer EC. Circ Res 1995;76:381–387. [PubMed: 7859384]
9. Laird DW, Puranam KL, Revel JP. Biochem J 1991;273:67–72. [PubMed: 1846532]
10. Musil LS, Cunningham BA, Edelman GM, Goodenough DA. J Cell Biol 1990;111:2077–2088. [PubMed: 2172261]
11. Traub O, Look J, Dermietzel R, Brummer F, Hulser D, Willecke K. J Cell Biol 1989;108:1039–1051. [PubMed: 2537831]
12. Beardslee MA, Laing JG, Beyer EC, Saffitz JE. Circ Res 1998;83:629–635. [PubMed: 9742058]
13. Fallon RF, Goodenough DA. J Cell Biol 1981;90:521–526. [PubMed: 7287816]
14. Beardslee MA, Lerner DL, Tadros PN, Laing JG, Beyer EC, Yamada KA, Kleber AG, Schuessler RB, Saffitz JE. Circ Res 2000;87:656–662. [PubMed: 11029400]
15. Girao H, Pereira P. Mol Vis 2003;9:24–30. [PubMed: 12567182]
16. Laing JG, Beyer EC. J Biol Chem 1995;270:26399–26403. [PubMed: 7592854]
17. Laing JG, Tadros PN, Westphale EM, Beyer EC. Exp Cell Res 1997;236:482–492. [PubMed: 9367633]
18. Musil LS, Le AC, VanSlyke JK, Roberts LM. J Biol Chem 2000;275:25207–25215. [PubMed: 10940315]
19. Fuertes G, Martin De Llano JJ, Villarroya A, Rivett AJ, Knecht E. Biochem J 2003;375:75–86. [PubMed: 12841850]
20. Qin H, Shao Q, Igdoura SA, Alaoui-Jamali MA, Laird DW. J Biol Chem 2003;278:30005–30014. [PubMed: 12767974]
21. Rutz ML, Hulser DF. Eur J Cell Biol 2001;80:20–30. [PubMed: 11211932]
22. Leithe E, Rivedal E. J Cell Sci 2004;117:1211–1220. [PubMed: 14970263]
23. VanSlyke JK, Musil LS. J Cell Biol 2002;157:381–394. [PubMed: 11980915]
24. Barker RJ, Price RL, Gourdie RG. Circ Res 2002;90:317–324. [PubMed: 11861421]

25. Toyofuku T, Yabuki M, Otsu K, Kuzuya T, Hori M, Tada M. J Biol Chem 1998;273:12725–12731. [PubMed: 9582296]
26. Toyofuku T, Akamatsu Y, Zhang H, Kuzuya T, Tada M, Hori M. J Biol Chem 2001;276:1780–1788. [PubMed: 11035005]
27. Giepmans BN, Verlaan I, Hengeveld T, Janssen H, Calafat J, Falk MM, Moolenaar WH. Curr Biol 2001;11:1364–1368. [PubMed: 11553331]
28. Lan Z, Kurata WE, Martyn KD, Jin C, Lau AF. Biochemistry 2005;44:2385–2396. [PubMed: 15709751]
29. Bertolaet BL, Clarke DJ, Wolff M, Watson MH, Henze M, Divita G, Reed SI. Nat Struct Biol 2001;8:417–422. [PubMed: 11323716]
30. Schauber C, Chen L, Tongaonkar P, Vega I, Lambertson D, Potts W, Madura K. Nature 1998;391:715–718. [PubMed: 9490418]
31. Biggins S, Ivanovska I, Rose MD. J Cell Biol 1996;133:1331–1346. [PubMed: 8682868]
32. Kim I, Mi K, Rao H. Mol Biol Cell 2004;15:3357–3365. [PubMed: 15121879]
33. Raasi S, Pickart CM. J Biol Chem 2003;278:8951–8959. [PubMed: 12643283]
34. Rao H, Sastry A. J Biol Chem 2002;277:11691–11695. [PubMed: 11805121]
35. Elsasser S, Gali RR, Schwickart M, Larsen CN, Leggett DS, Muller B, Feng MT, Tubing F, Dittmar GA, Finley D. Nat Cell Biol 2002;4:725–730. [PubMed: 12198498]
36. Wilkinson CR, Seeger M, Hartmann-Petersen R, Stone M, Wallace M, Semple C, Gordon C. Nat Cell Biol 2001;3:939–943. [PubMed: 11584278]
37. Bertolaet BL, Clarke DJ, Wolff M, Watson MH, Henze M, Divita G, Reed SI. J Mol Biol 2001;313:955–963. [PubMed: 11700052]
38. Chen L, Shinde U, Ortolan TG, Madura K. EMBO Rep 2001;2:933–938. [PubMed: 11571271]
39. Chen L, Madura K. Mol Cell Biol 2002;22:4902–4913. [PubMed: 12052895]
40. Funakoshi M, Sasaki T, Nishimoto T, Kobayashi H. Proc Natl Acad Sci U S A 2002;99:745–750. [PubMed: 11805328]
41. Jin, C.; Lau, AF. Characterization of a Novel SH3-containing Protein That May Interact with Connexin43. IOS Press; Amsterdam, The Netherlands: 1998. p. 230-234.
42. Jin C, Lau AF, Martyn KD. Methods 2000;20:219–231. [PubMed: 10671315]
43. Hollenberg SM, Sternglanz R, Cheng PF, Weintraub H. Mol Cell Biol 1995;15:3813–3822. [PubMed: 7791788]
44. Davidson JD, Riley B, Burright EN, Duvick LA, Zoghbi HY, Orr HT. Hum Mol Genet 2000;9:2305–2312. [PubMed: 11001934]
45. Roth AF, Sullivan DM, Davis NG. J Cell Biol 1998;142:949–961. [PubMed: 9722608]
46. Mueller TD, Feigon J. EMBO J 2003;22:4634–4645. [PubMed: 12970176]
47. Ortolan TG, Tongaonkar P, Lambertson D, Chen L, Schauber C, Madura K. Nat Cell Biol 2000;2:601–608. [PubMed: 10980700]
48. Voges D, Zwickl P, Baumeister W. Annu Rev Biochem 1999;68:1015–1068. [PubMed: 10872471]
49. Abriel H, Kamynina E, Horisberger JD, Staub O. FEBS Lett 2000;466:377–380. [PubMed: 10682864]
50. Thomas MA, Zosso N, Scerri I, Demaurex N, Chanson M, Staub O. J Cell Sci 2003;116:2213–2222. [PubMed: 12730291]
51. Lambertson D, Chen L, Madura K. Curr Genet 2003;42:199–208. [PubMed: 12589471]
52. Hiyama H, Yokoi M, Masutani C, Sugasawa K, Maekawa T, Tanaka K, Hoeijmakers JH, Hanaoka F. J Biol Chem 1999;274:28019–28025. [PubMed: 10488153]
53. Kleijnen MF, Alarcon RM, Howley PM. Mol Biol Cell 2003;14:3868–3875. [PubMed: 12972570]
54. Verma R, Oania R, Graumann J, Deshaies RJ. Cell 2004;118:99–110. [PubMed: 15242647]
55. Bedford FK, Kittler JT, Muller E, Thomas P, Uren JM, Merlo D, Wisden W, Triller A, Smart TG, Moss SJ. Nat Neurosci 2001;4:908–916. [PubMed: 11528422]
56. Elsasser S, Chandler-Militello D, Muller B, Hanna J, Finley D. J Biol Chem 2004;279:26817–26822. [PubMed: 15117949]
57. Saeki Y, Saitoh A, Toh-e A, Yokosawa H. Biochem Biophys Res Commun 2002;293:986–992. [PubMed: 12051757]

58. Elsasser S, Finley D. Nat Cell Biol 2005;7:742–749. [PubMed: 16056265]
59. Matsuda M, Koide T, Yorihuzi T, Hosokawa N, Nagata K. Biochem Biophys Res Commun 2001;280:535–540. [PubMed: 11162551]
60. Meusser B, Hirsch C, Jarosch E, Sommer T. Nat Cell Biol 2005;7:766–772. [PubMed: 16056268]
61. Romisch K. Annu Rev Cell Dev Biol 2005;21:435–456. [PubMed: 16212502]
62. Abriel H, Loffing J, Rebhun JF, Pratt JH, Schild L, Horisberger JD, Rotin D, Staub O. J Clin Invest 1999;103:667–673. [PubMed: 10074483]
63. Schwake M, Friedrich T, Jentsch TJ. J Biol Chem 2001;276:12049–12054. [PubMed: 11116157]
64. Staub O, Dho S, Henry P, Correa J, Ishikawa T, McGlade J, Rotin D. EMBO J 1996;15:2371–2380. [PubMed: 8665844]
65. Leithe E, Rivedal E. J Biol Chem 2004;279:50089–50096. [PubMed: 15371442]
66. Leykauf K, Salek M, Bomke J, Frech M, Lehmann WD, Durst M, Alonso A. J Cell Sci 2006;119:3634–3642. [PubMed: 16931598]
67. Laing JG, Tadros PN, Green K, Saffitz JE, Beyer EC. Cardiovasc Res 1998;38:711–718. [PubMed: 9747439]

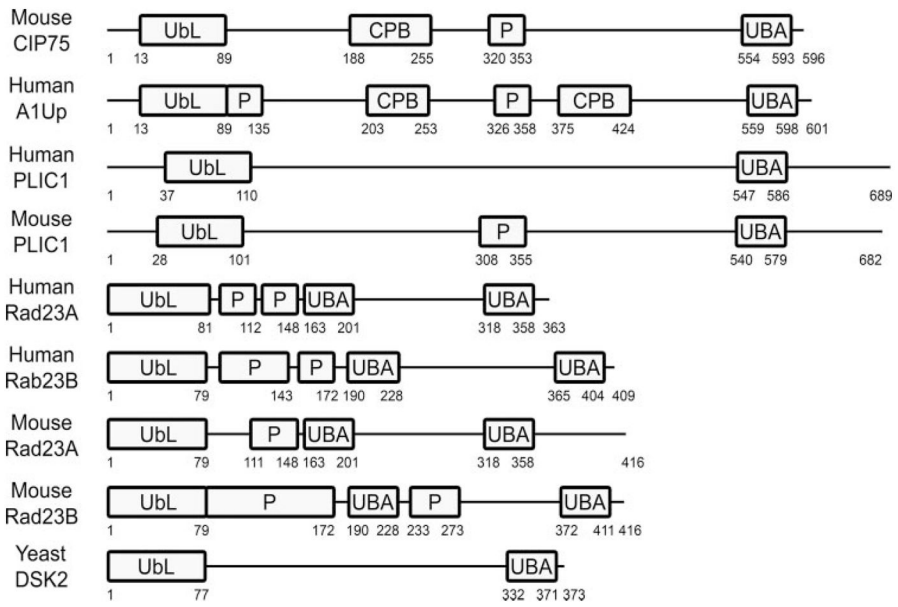

FIGURE 1. Domain structure of CIP75 and other UbL-UBA domain-containing proteins

CIP75 contains 596 amino acids and has a single ubiquitin-like domain (*UbL*) at its N terminus and an ubiquitin-associated (*UBA*) domain located at its C-terminal tail. CIP75 also has a PEST (*P*) sequence and a heat shock chaperonin-binding (*CPB*) domain. The general structures of the human A1Up, human and mouse PLIC1, human and mouse Rad23A, Rad23B, and yeast DSK2 proteins are shown for comparison.

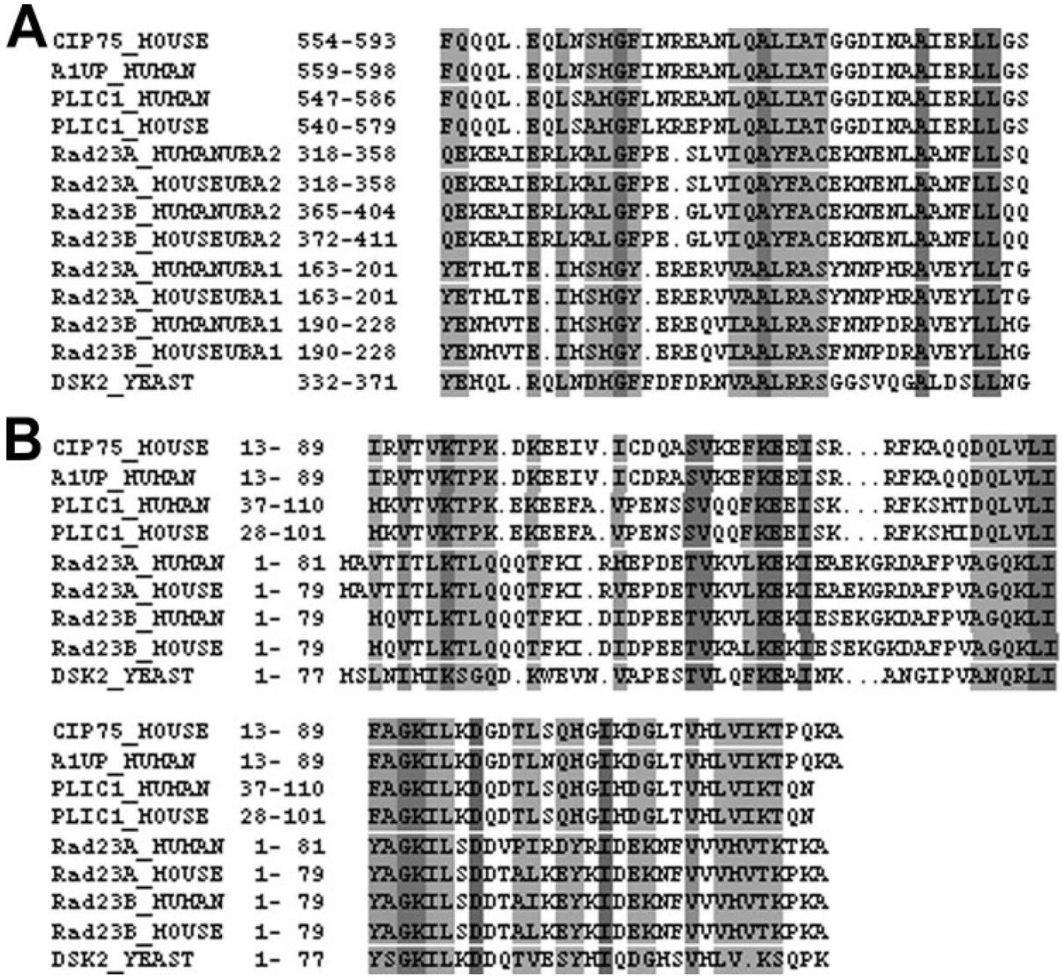

FIGURE 2. Amino acid sequence alignments of the UBA and UbL domains of CIP75 and other UbL-UBA domain-containing proteins

Amino acid sequence alignment of the UBA domains (*A*) and the UbL domains (*B*) of mouse CIP75, human A1Up, human and mouse PLIC1, human and mouse Rad23A, Rad23B, and yeast DSK2 proteins. The *numbers* in *A* and *B* represent the amino acid positions from the N to C termini. The *shading gradient* denotes the degree of identity or similarity, the darker the color, the higher homology among the proteins.

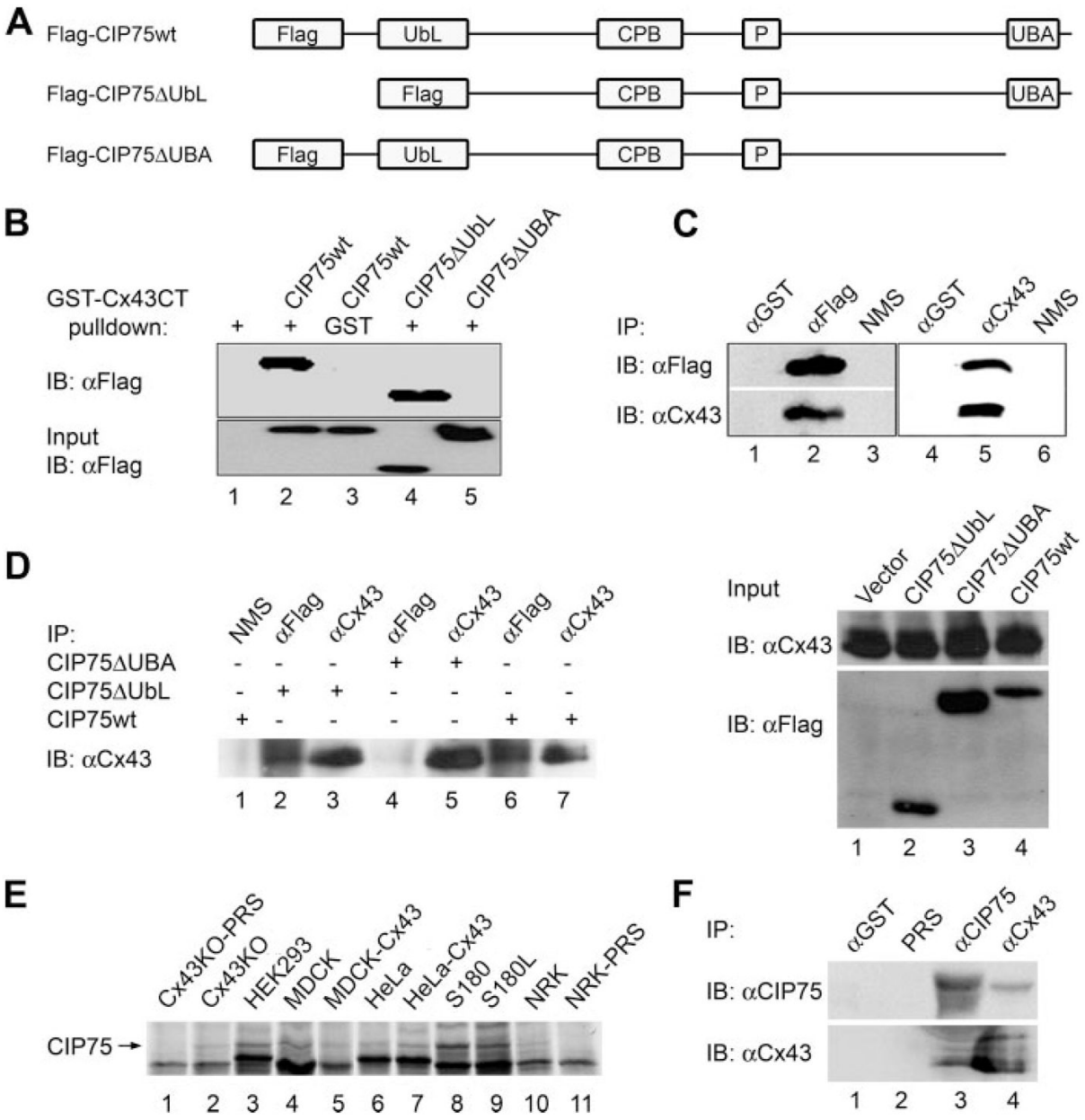

FIGURE 3. The interaction between Cx43 and CIP75 is dependent upon the UBA domain of CIP75

A, schematic diagram of FLAG-CIP75wt and the FLAG-CIP75 UbL (FLAG-CIP75ΔUbL) and FLAG-CIP75 UBA (FLAG-CIP75ΔUBA) deletion mutants. *B*, GST-Cx43CT was bacterially expressed, purified, and mixed with bacteria lysates containing FLAG-CIP75wt, FLAG-CIP75ΔUbL, or FLAG-CIP75ΔUBA. Proteins bound to the GST-Cx43CT were collected on glutathione-agarose beads and analyzed by immunoblotting with anti-FLAG. *Top*: GST pulldown assays with GST-Cx43CT only (*lane 1*), GST-Cx43CT and FLAG-CIP75wt (*lane 2*), GST only and FLAG-CIP75wt (*lane 3*), GST-Cx43CT and FLAG-CIP75ΔUbL (*lane 4*), and GST-Cx43CT and FLAG-CIP75ΔUBA (*lane 5*). *Bottom*: input of FLAG tagged-CIP75wt (*lanes 2* and *3*), FLAG-CIP75ΔUbL (*lane 4*), and FLAG-CIP75ΔUBA (*lane 5*). *C*, transiently expressed Cx43 and FLAG-CIP75 in HEK293 cells were co-immunoprecipitated. Cell lysates were immunoprecipitated with anti-GST (*lanes 1* and *4*), anti-

FLAG (*lane 2*), normal mouse serum (NMS, *lanes 3* and *6*), and Cx43 antibody (*lane 5*). Co-immunoprecipitated Cx43 or CIP75 were detected by immunoblotting using anti-Cx43 or anti-FLAG, respectively. *D*, transiently expressed FLAG-CIP75wt or the FLAG-CIP75 deletion mutants in HeLa-Cx43 cells were co-immunoprecipitated with Cx43. *Left*: cell lysates containing FLAG-CIP75wt (*lanes 1*, *6*, and *7*), FLAG-CIP75ΔUbL (*lanes 2* and *3*), or FLAG-CIP75ΔUBA (*lanes 4* and *5*) were immunoprecipitated with normal mouse serum (*lane 1*), FLAG antibody (*lanes 2*, *4*, and *6*), or Cx43 antibody (*lanes 3*, *5*, and *7*). *Right*: expression and loading controls for HeLa-Cx43 cells transiently transfected with FLAG-CIP75wt or the FLAG-CIP75 deletion mutants: vector only control (*lane 1*), FLAG-CIP75ΔUbL (*lanes 2*), FLAG-CIP75ΔUBA (*lane 3*), and FLAG-CIP75wt (*lane 4*). Cx43 or CIP75 were detected by immunoblotting using anti-Cx43 or anti-FLAG, respectively. *E*, expression of endogenous CIP75 in Cx43KO, HEK293, MDCK, MDCK-Cx43, HeLa, HeLa-Cx43, S180, S180L and NRKe cells. Endogenously expressed CIP75 was detected by the immunoprecipitation of [^{35}S]methionine/cysteine-labeled cell lysates with anti-CIP75 (*lanes 2–10*) and compared with immunoprecipitation using preimmune rabbit serum (PRS: *lanes 1* and *11*). *F*, endogenously expressed Cx43 and CIP75 in MDCK-Cx43 cells were co-immunoprecipitated. Cell lysates were immunoprecipitated with anti-GST (*lane 1*), preimmune rabbit serum (*lane 2*), anti-CIP75 (*lane 3*), or anti-Cx43 (*lane 4*). The immunoprecipitated proteins were immunoblotted with either anti-CIP75 (*top*) or anti-Cx43 (*bottom*).

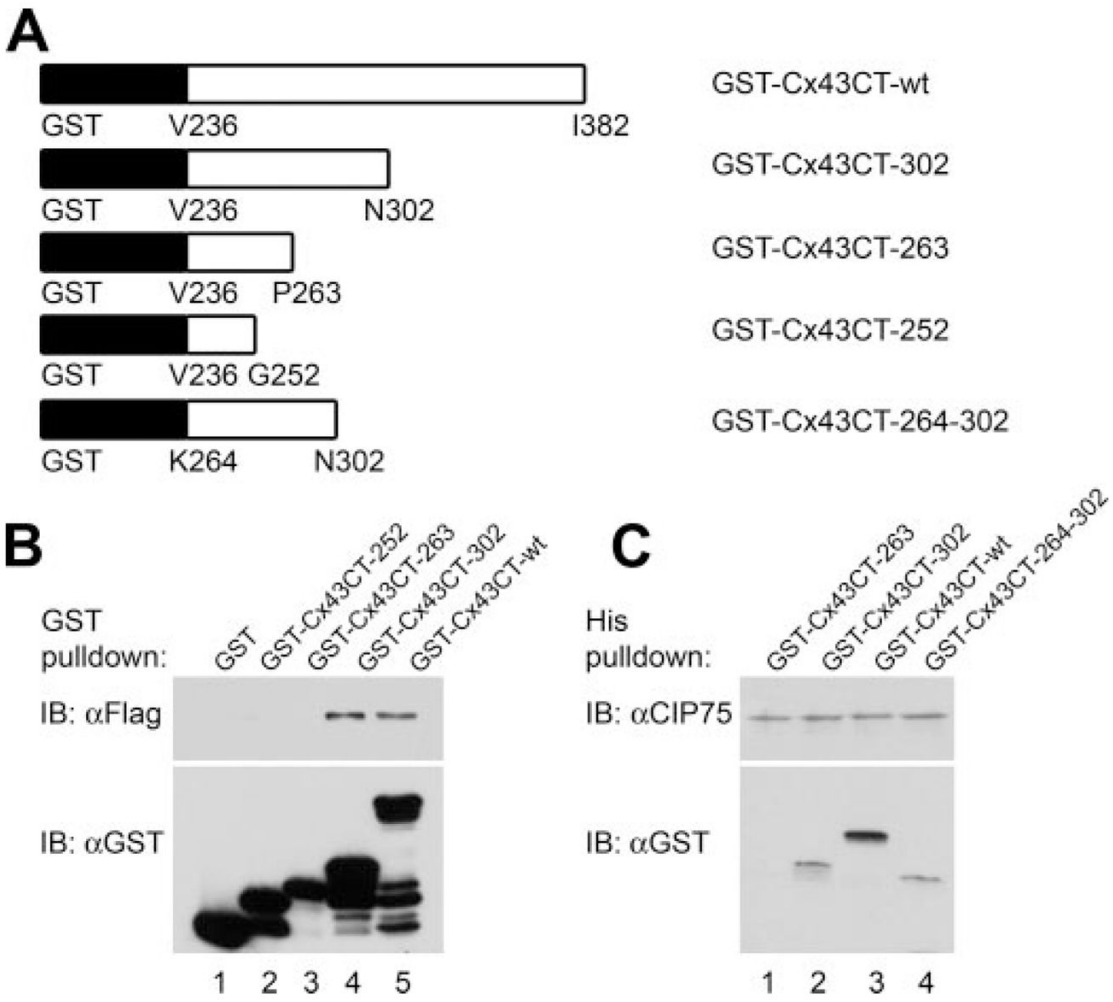

FIGURE 4. The region between Lys^{264}–Asn^{302} of Cx43 is necessary for binding to CIP75

A, schematic representation of the different GST-fused Cx43CT deletion mutants used in *in vitro* pulldown binding assays against CIP75. *B* and *C*, GST and His pulldown assays of FLAG-CIP75 (in pET28a vector containing His tag). GST alone, GST-Cx43CT-wt, GST-Cx43CT deletion mutants, or FLAG-CIP75 were expressed in bacteria. *B*, *top*: lysates containing FLAG-CIP75 were incubated with GST alone (*lane 1*), GST-Cx43CT-wt (*lane 5*), or the GST-Cx43CT deletion mutants (*lanes 2– 4*) purified on glutathione-agarose beads. The amount of FLAG-CIP75 specifically bound to the GST-Cx43 was analyzed by immunoblotting with anti-FLAG. *Bottom*: expression levels of the GST alone, GST-Cx43CT-wt, and the GST-Cx43CT deletion mutants in bacteria were determined by immunoblotting with anti-GST. *C*, lysates containing GST-Cx43CT-wt (*lane 3*) or GST-Cx43CT deletion mutants (*lanes 1*, *2*, and *4*) were incubated with His-FLAG-CIP75 purified on cobalt beads. *Top*: the amount of CIP75 bound to beads was determined by immunoblotting with anti-CIP75. *Bottom*: the amount of GST-Cx43-wt and the GST-Cx43CT deletion mutants that bound to CIP75 was analyzed by immunoblotting with anti-GST.

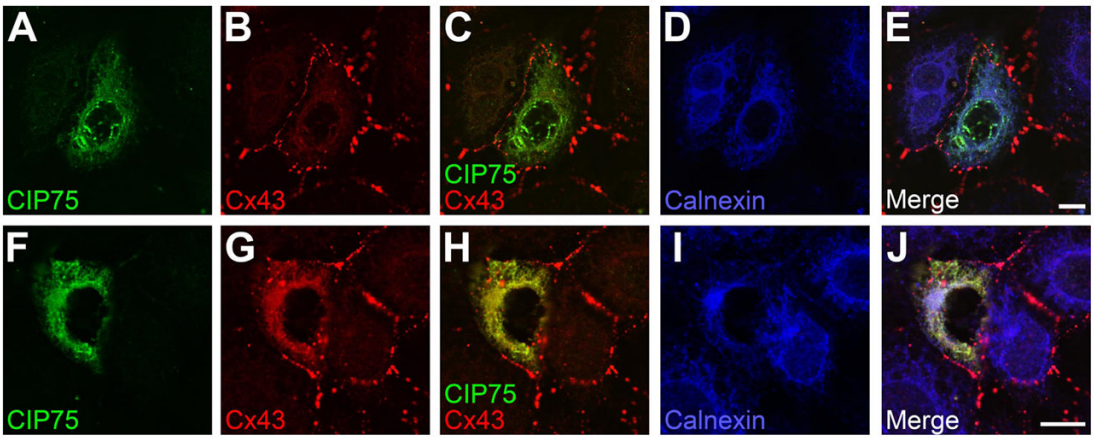

FIGURE 5. CIP75 and Cx43 co-localize at the ER

NRKe cells were transiently transfected with FLAG-CIP75. The subcellular localization of CIP75 (*green*, *A* and *F*) and Cx43 (*red*, *B* and *G*) with the ER marker calnexin (*blue*, *D* and *I*) was visualized by LSCM. CIP75 expression causes increased levels of cytoplasmic Cx43 to varying degrees (*top*, lower levels; *bottom*, higher levels) where CIP75 co-localizes with Cx43 (*yellow*, *C* and *H*). CIP75 and Cx43 co-localization occurs at or around the ER (*E* and *J*). *Scale bar*: 10 μm.

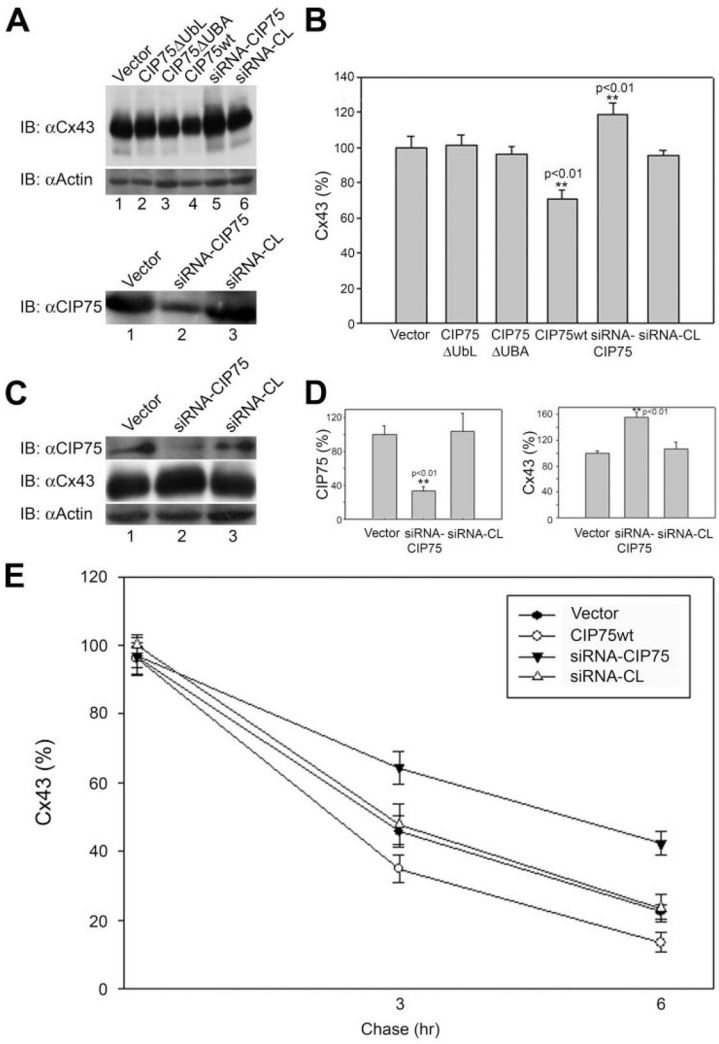

FIGURE 6. CIP75 affects the degradation of Cx43

A, HeLa-Cx43 cells were transiently transfected with vector only (*lane 1*), FLAG-CIP75ΔUbL (*lane 2*), FLAG-CIP75ΔUBA (*lane 3*), FLAG-CIP75wt (*lane 4*), siRNA-CIP75 (*lane 5*), or siRNA-CL (*lane 6*). Cells were lysed after 48 h, and total cell lysates were analyzed by immunoblotting with anti-Cx43 (*top panel*). Immunoblotting for actin served as a loading control (*middle panel*). HeLa-Cx43 cells were transfected with vector only, siRNA-CIP75, or siRNA-CL, and lysed after 48 h. Expression of CIP75 was analyzed by immunoblotting with anti-CIP75 (*bottom panel*). *B*, Cx43 protein levels, normalized to the vector-only control, were quantified usingaBio-RadFluor-SMultiImagerandanalyzedwithQuantityOnesoftware. Thedatarepresentthemeanofthree independent experiments ±S.E. **, represents average Cx43 values with statistically significant differences (p <0.01) from the vector-only control value. *C*, S180 cells were transfected with vector only (*lane 1*), CIP75 siRNA (siRNA-CIP75, *lane 2*), or a random siRNA control (siRNA-CL, *lane 3*) and incubated for 48 h. Amounts of CIP75 and Cx43 were assayedbyimmunoblottingwithanti-CIP75andanti-Cx43(*top* and*middle panels*). Immunoblottingforactinserved as a loading control (*bottom panel*). *D*, quantitative analysis of CIP75 (*left panel*) and Cx43 (*right panel*) following the introduction of CIP75 siRNA into S180 cells. The data represent the means of three independent experiments ±S.E. **, represents average CIP75 or Cx43 values with statistically-significant differences (p <0.01) from the vector-only control value. *E*, HeLa-Cx43 cells were transiently transfected with vector

only, CIP75wt, siRNA-CIP75, or siRNA-CL, incubated for 48 h, labeled with [^{35}S]methionine/cysteine for 1 h, followed by a chase of 3 or 6 h. Cell lysates were immunoprecipitated with anti-Cx43, resolved by SDS-PAGE, and the proteins was analyzed with Bio-Rad phosphorimaging device. The data represent the means of at least three independent experiments ±S.E. The *y*-axis represents the percentage of the radiolabeled Cx43 remaining after the 3- or 6-h chase.

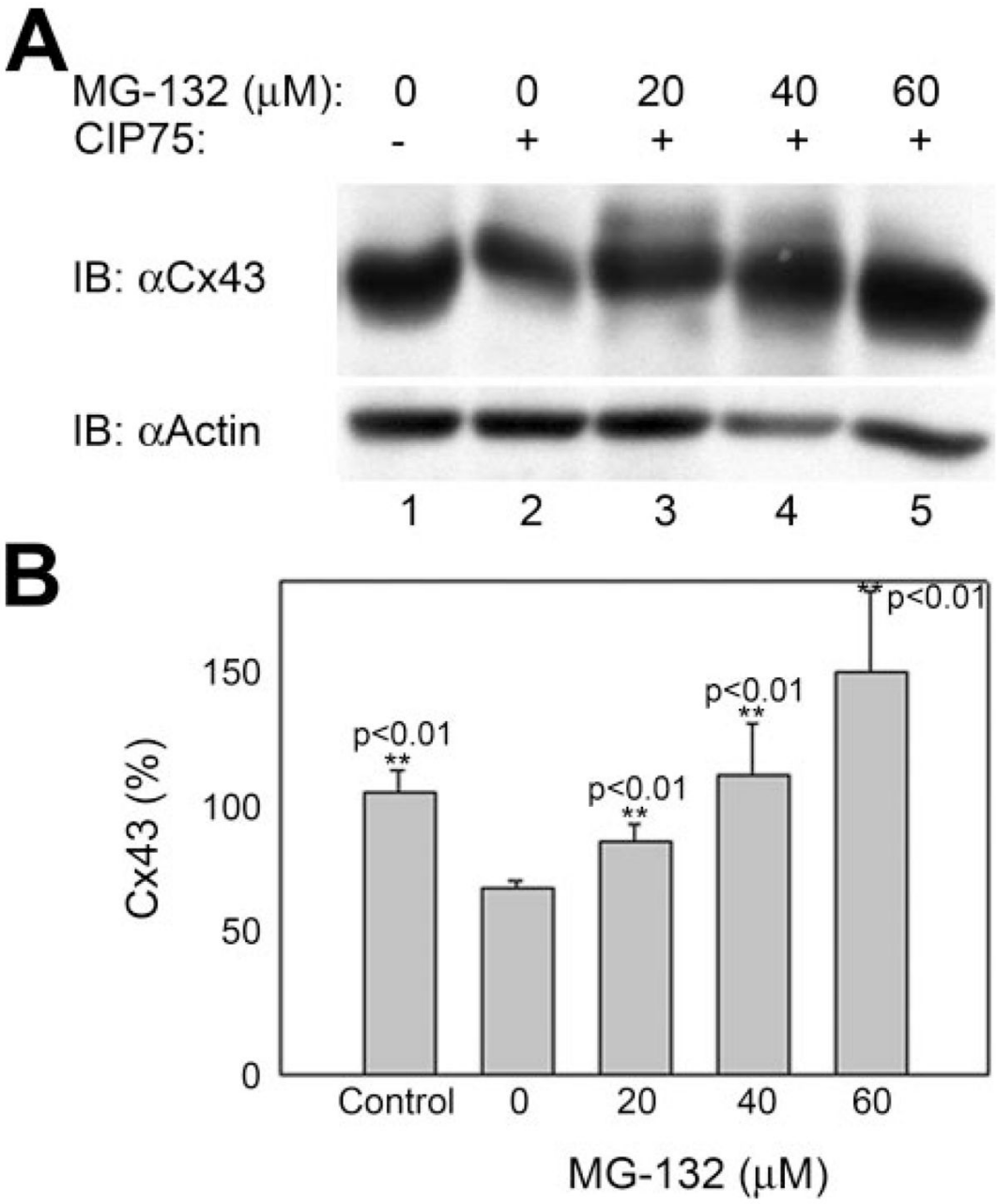

FIGURE 7. CIP75 may affect Cx43 degradation through the proteasome degradation pathway

A, HeLa-Cx43 cells were transfected with vector only or CIP75wt, incubated for 24 h, then treated with the proteasomal inhibitor, MG-132, at 20, 40, or 60 μ_M for 4 h. Lysate proteins were analyzed by immunoblotting with anti-Cx43 (*top*) with actin as a loading control (*bottom*). *B*, quantitative analysis of Cx43 in absence or presence of MG-132. The data represent the means of three independent experiments ±S.E. **, represents average Cx43 values with statistically significant differences (p <0.01) between either the vector-only control and CIP75wt transfected cells or the untreated *versus* MG-132-treated CIP75wt transfected cell values.

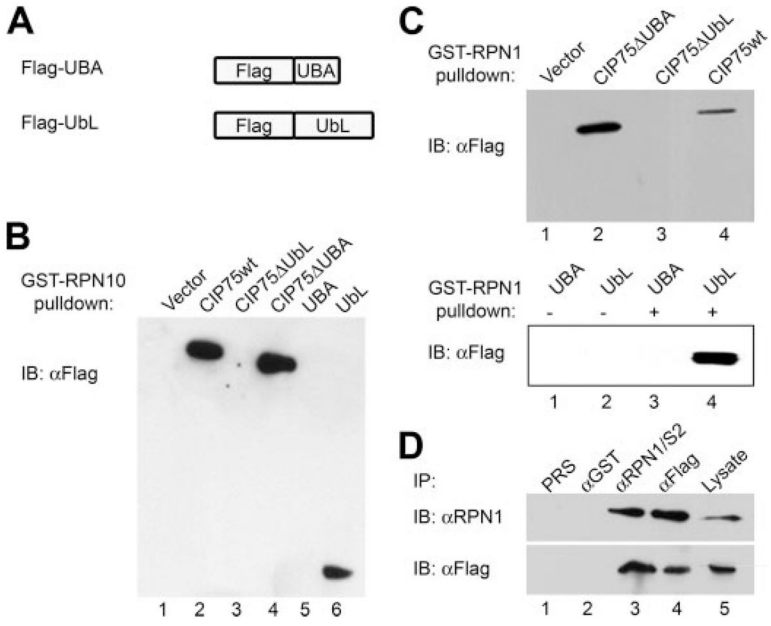

FIGURE 8. CIP75 interacts with the RPN10/S5a and RPN1/S2 proteins of 19 S proteasomal subunit through its UbL domain

A, schematic diagram of the FLAG-UBA and FLAG-UbL fusion proteins. *B*, GST-RPN10/S5a was expressed in and purified from bacteria, mixed with lysates of bacteria expressing vector only (*lane 1*), FLAG-CIP75wt (*lane 2*), FLAG-CIP75ΔUbL (*lane 3*), FLAG-CIP75ΔUBA (*lane 4*), FLAG-UBA (*lane 5*), or FLAG-UbL (*lane 6*). The proteins were collected on glutathione-agarose beads and analyzed by immunoblotting with anti-FLAG. *C*, GST-RPN1/S2 was expressed in and purified from bacteria, mixed with lysates of bacteria transformed with (*top*) vector alone (*lane 1*), FLAG-CIP75ΔUBA (*lane 2*), FLAG-CIP75ΔUbL (*lane 3*), or FLAG-CIP75wt (*lane 4*). *Bottom*: lysates of bacteria transformed with FLAG-UBA (*lanes 1* and *3*) or FLAG-UbL (*lanes 2* and *4*) were mixed with purified GST-RPN1/S2 in pull-down assays. Isolated proteins were analyzed with anti-FLAG as described in *B*. *D*, HeLa-Cx43 cells were transiently transfected with FLAG-CIP75 for 24 h and the cell lysates were immunoprecipitated with preimmune serum (PRS, *lane 1*), anti-GST (*lane 2*), anti-RPN1 (*lane 3*), or anti-FLAG (*lane 4*). The immunoprecipitates were blotted with the reciprocal anti-RPN1 (*top*) or anti-FLAG for CIP75 (*bottom*). Expression levels of RPN1/S2 or FLAG-CIP75 in transiently transfected HeLa-Cx43 cell lysates are shown in *lane 5*.